Int. J. Electrochem. Sci., 11 **(2016)** 4957 – 4965, doi: 10.20964/2016.06.80

International Journal of
ELECTROCHEMICAL
SCIENCE
www.electrochemsci.org

Short Communication

Corrosion Performance of a Novel NiAl-Cu Intermetallic HVOF Protective Coating Part II: High Temperature Corrosion in Molten Salts

E. F. Díaz[1,2], *A. M. Ramirez-Arteaga*[1,2], *S. Serna*[1,*], *A. Torres*[2], *A. Molina*[1], *M.A. Lucio-García*[3], *J. Colin*[2]

[1]Centro de Investigación en Ingeniería y Ciencias Aplicadas - UAEM, Av. Universidad 1001, Chamilpa 62209, Cuernavaca, Morelos, México.
[2]Facultad de Ciencias Químicas e Ingeniería, Programa Educativo de Ingeniería Mecánica - UAEM.
[3] Facultad de Química, Universidad Autónoma de Yucatán - C. 43 No. 613 x C. 90, Inalámbrica 97069, Mérida, Yucatán, México.
[*]E-mail: aserna@uaem.mx

Received: 20 January 2016 / *Accepted:* 17 March 2016 / *Published:* 4 May 2016

High temperature localized corrosion is one of the most hazardous corrosion form producing fast and unanticipated destruction into a small section of a metal structure. Electrochemical Noise (EN) is an electrochemical technique providing rate and corrosion mechanism of corrosion in-situ process. Amplitude fluctuations intensities are associated to corrosion process that can be observed in electrochemical noise measurements (ENMs) and their shape related with the type of corrosion process. For corrosion the electrochemical noise signals (ENS) consist on a high overlapped transient therefore they need appropriated mathematical treatment. Since 1990 the wavelet analysis proposed as a mathematical tool for signal processing alternative to Fourier transform when a precise time-scale analysis is required or to study transients into a signal. For the present study the EN technique was used to monitor the corrosion of a NiAl+Cu Intermetallic HVOF protective coating of Inconel alloy 600 at 750 °C in molten salts. The Discrete Wavelet Transform (DWT) technique was used for treating noise signal from respective transients and detect highly localized pitting corrosion. The original potential and current noise were first disintegrated into a series of time k by DWT at increasing scale j. Then, the noise resistance $R_n(j)$ was calculated as a ratio of the standard deviation of the reconstructed potential noise to the reconstructed current noise. The experimental results demonstrated that the DWT technique could improve the calculation of the classic noise resistance $R_{sn}(f)$ because it can remove the low frequency trend coupled in the potential or current fluctuations very well.

Keywords: Wavelet analysis; Electrochemical noise; High temperature corrosion.

1. INTRODUCTION

Commercial alloys Cu-Ni base are very corrosion resistant in various aggressive environments, which suggests that this type of alloy has very promising corrosive properties [1]. Unfortunately its production by conventional thermal methods becomes complex due to the large difference in their melting points. The alloys that are currently used for high temperature applications are usually made from iron, nickel or cobalt because such alloys have a high melting point.

Intermetallic compounds are promising materials as may be applied in a wide range of technology areas [2]. The most important characteristics that have this type of alloys is that they are highly resistance corrosion, have low density, which combined with their ability to retain strength and stiffness at elevated temperatures [3, 4]. It has been reported in the literature, research system intermetallic Ni-Al [5]. But, this system is not yet available in structural applications. Intermetallic compound in Ni-Al systems, together with γ'-Ni_3Al, haves been used as a coating material for Ni-base superalloys, because of its excellent oxidation resistance conditions.

In the industry of energy production, the performance of the boilers and other equipments, reduce its lifetime because the products of combustion deteriorate the materials used in these devices. Compounds such as vanadium and sulfur accelerate oxidation processes, coupled with this high operating temperature. This condition also increases the generation of SO_3 and hence the corrosion by sulfuric acid in the low temperature zone of the boiler [6]. Here intermetallic NiAlCu type materials was thought to be successful in order to withstand the high temperature corrosion as a coating for Ni base superalloys applied by HVOF deposition technique.

On the other hand, electrochemical noise measurements (ENM) provide information of corrosion mechanisms, so this technique was eligible to monitor the NiAlCu coating hot corrosion process. The amplitude of the fluctuations observed in electrochemical noise records (ENR) can be correlated with the intensity of the corrosion process, while the fluctuation shape observed in these records can be associated with the type of corrosion process [7]. According to A. Aballe et al. electrochemical noise analysis often requires appropriate mathematical tools. Statistical methods have been proposed, based on spectral and other chaos theory. Bertocci et al. [8, 9] suggested that due to the inhomogeneity of the test electrodes during the ENMs it was possibly to cause a low frequency trend or DC trend coupled in the potential or current fluctuation which will produce $1/f2$ slopes in the PSD plots.

Furthermore, Mansfeld et al. [10] says that the standard deviation of fluctuations in the potential (σV) and current (σI), could change, affecting directly the values of noise resistance, which is given by the relationship $R_n = \sigma V/\sigma I$ [11, 12, 13]. Y. J. Tan et al. [14] used a method to the removal the trend called Moving Average Removal (MAR). The idea behind this is to remove, using the method MAR, the average noise values from the record. Later, Mansfeld proposed the method named Liner Removal Trend (LTR) in order to obtain a better removal trend.

Recently a mathematical tool developed several years ago called discrete wavelet transform (DWT) was applied for this purpose. Since one of the disadvantages of statistical methods is that they analyze signals by averaging the features across the whole time record, the discrete wavelet transform (DWT) has been proposed as a method of analysis that meets the aforementioned limitations under hot corrosion phenomena. The aim of this paper is to show that by analyzing wavelet, it can get a better relationship between the parameter called electrochemical noise resistance $R_n(j)$ at different decomposition scale and the scale.

2. WAVELET BACKGROUND

The wavelet transform is a tool that cuts up data or functions or operators into different frequency components, those different frequency components can be study with a resolution matched to its frequency. The wavelet transform of a signal involves two variables: (frequency); so that the wavelets can provide a tool for time-frequency localization.

Let us consider a time record x_n, *(n=1, 2, 3,..., N)* which is expressed on the Cartesian basis. The DWT approach consists in expressing the time record as $x_n(t)$, using a linear combination of base functions oscillating ϕ_{jk} (t) and ψ_{jk} (t); of a limited span of time:

$$x(t) = \sum_k S_{J,k}\phi_{J,k}(t) + \sum_k d_{J,k}\psi_{J,k}(t) + \sum_k d_{J-1,k}\psi_{J-1,k}(t) + \sum_k d_{1,k}\psi_{1,k}(t) \quad (1)$$

Where $S_{J,k}$, $d_{J,k}$,…,$d_{1,K}$, are the so-called wavelet coefficient; J is a small number which depends mainly of N and the base functions; and k ranges from 1 to the number of coefficients in the specified component. The coefficients $S_{J,k}$ are called the smooth coefficients because they contain the information about the general trend of the signal, and $d_{j,K}$ *(I= 1, 2, 3,...,J)* are named the detail coefficients, which contain information about the local fluctuations of the series. The base functions ϕ_{jk} (t) and ψ_{jk} (t) are generated from the mother ϕ (t) and father ψ (t) wavelet trough the scaling and translation equations, given by:

$$\phi_{jk}(t) = 2^{-j/2}\phi\left(\frac{t-2^{jk}}{2^j}\right) \qquad \psi_{jk}(t) = 2^{-j/2}\psi\left(\frac{t-2^{jk}}{2^j}\right) \quad (2)$$

Where *(k = 1, 2, 3,..., N/2^J)* and j = 1, 2, 3,…,J. Notice that 2^j act as scale factor and 2^{jk} as translation parameter.

3. EXPERIMENTAL PROCEDURE

The coating process of the NiAlCu intermetallic over the Ni superalloy substrate was detailed elsewhere [17-19]. The Ni superalloy substrate coated with NiAlCu samples were cut to obtain 10x10mm flat squares surfaces with 1 mm thickness. Two coated sample was welded on one of its sides to nicromel wire (80Cr-20Ni) taking care that the coated side was in contact to molten salts. Every single welded samples were placed inside a ceramic tube with dimensions of 8.09 mm of outer diameter, 5.00 mm inner diameter and 200 mm in length. Each the tube was sealed in the coated sample part at one end of the tubes with refractory cement. ENM data were obtained with two identical coated sample electrodes and one platinum wire as reference electrode arrangement. Both potential and current noise signals were measured simultaneously, at open circuit potential.

This arrangement was then installed in a vertical electric furnace and introduced in a ceramic crucible which contains a mixture of 0.5 M NaCl + Na_2SO_4, which was maintained at a constant temperature of 750°C ± 4°C during the test period. The temperature inside the furnace was monitored by a K type thermocouple, which in turn is connected to an analog meter.

Measurements were carried out, a Gill AC from ACM Instruments was used, controlled using a desktop computer. Taking readings in blocks of 1024 points taken at 1 s interval. The wavelet analysis was carried out by MATLAB 7.8 software.

4. RESULTS AND DISCUSSION

4.1. Spectral Analysis

After 12h of inmersion of the NiAl-Cu intermetallic HVOF protective coating in a molten salts at 750°C, typical potential and current fluctuations are shown in Fig. 1. It can see that the current noise transients as well noise transients present potential repetition frequencies with amplitudes of $12X10^{-5}$µA y 20mV, respectively. As it can be observed both the potential and the current fluctuations are very regular and occur in phase with each other, that is, their fluctuations always occur simultaneously. Also, there are many transients generated due to the great activity in the working electrodes which generates the beginning of metastable pits.

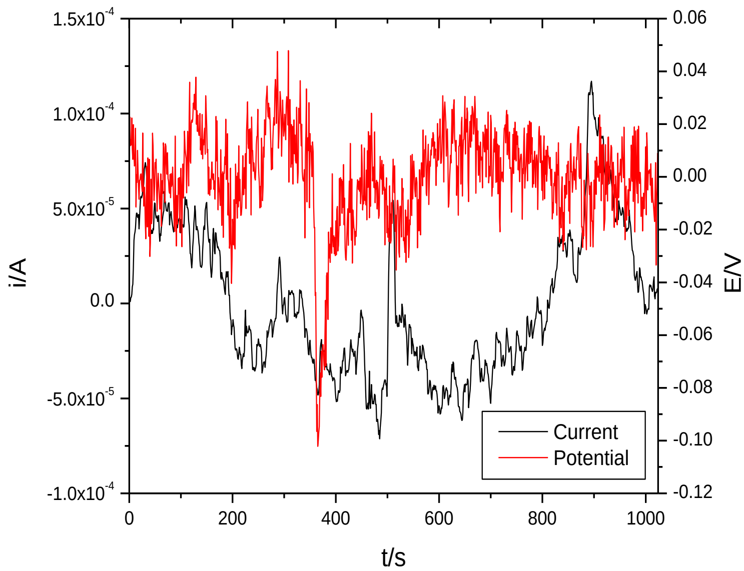

Figure 1. Electrochemical Noise (ECN).

Spectral Noise Resistance (R_{sn}) is defined as the square root of the potential noise PDS to that of current noise PDS at a particular frequency, and has been linked to the electrochemical equivalent impedance of the material under study, providing information about of corrosion rate [15]. In this paper, the spectral noise resistance studied by Mansfeld et al. [14] was calculated from the data electrochemical noise shown in Fig. 1, and is plotted in the fig. 2 (without mean removal and Hanning window yet) as a function of frequency (Hz) taken after 12 h of inmersion of the intermetallic HVOF protective coating in molten salts. It is observed that R_{sn} tending to 10K Ω. It is also noted that between 0.1 and 1 Hz (region where corrosion processes occur) the current decreases then increased above the primitive values, shows an increase in the noise level in the high frequency range. The slope of the density noise power spectral potential provides information about the type of corrosion and the slope of the power spectral density of the noise intensity reports on the process speed, in this case the slope remains more or less constant, with variations in amplitude, where you are, are associated with low porosity corrosion products and a less active surface, which is possibly related to a type of localized corrosion on the surface of the material , which generates corrosion products , which reduce the corrosion rate , favoring this a less active surface.

The method most frequently used to understand ENRs is by the study of PDS plots analyzed with fast Fourier Transform (FFT).

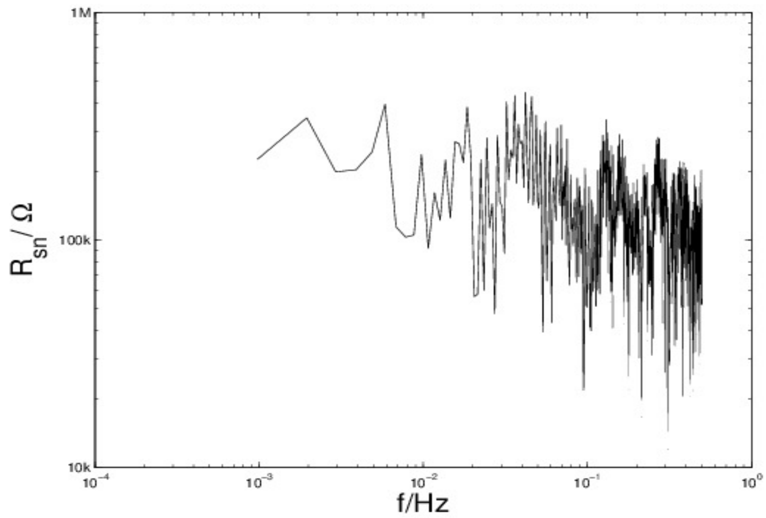

Figure 2. Spectral Noise Resistance

However, wavelet transform is more appropriate than Fourier transform to analyze signals with topographies that variate over time, and signals that comprise abrupt jumps or other non-smooth traits [16]. So, it come to be stimulating to parallel the relative potentials of Fourier and wavelet transforms. Then, another mode of representing the wavelet transform results becomes appropriated. For this exemplification a parameter, E_j, named the relative energy of a crystal, is plotted versus the crystal name. This plot is the energy distribution plot (EDP).

The EPDs are signals ‘fingerprints‘ as the PSD plots. Subsequently, it is likely to argue the Fourier and wavelet transform capabilities by matching PSD and EDP corresponding to the same ENR.

4.2. Wavelet Analysis.

To start with wavelet analysis method, it is necessary to eliminate the tendency, ie DWT estimate for each times series. The boundary conditions neccesary to perform DWT in this paper are those that consider that wavelet are zero outside the range of the time record [7, 12, 13]. This condition limits the type of wavelet that can be choosed to the symmlets wavelets [10].

A way of representing the results of DWT is estimating the contribution of each coefficients decomposition to the overall signal. The overall power of the signal or energy is calculated with the aid of the following equation [22],

$$E = \sum_{n=1}^{N} x_n^2 \qquad n = 1, \dots, N \tag{3}$$

The fraction of energy associated a each detail of the coefficient decomposition *j* is calculated as follows,

$$E_j^d = \frac{1}{E} \sum_{n=1}^{N/2^j} d_{j,n}^2 \qquad j = 1, \dots, J \tag{4}$$

for smooth coefficient at level *j* the equation is similar,

$$E_j^s = \frac{1}{E} \sum_{n=1}^{N/2^j} s_{j,n}^2 \tag{5}$$

Because the symmlet wavelets are orthogonal, the following equation should be is satisfied:

$$\sum_{n=1}^{N} x_n^2 = \sum_{j=1}^{J} \sum_{n=1}^{N/2^j} d_{j,n}^2 + \sum_{n=1}^{N/2^j} s_{j,n}^2 \tag{6}$$

In Fig. 3, it plots the relative energy accumulated E_j^d or E_j^s by each level decomposition versus *j* until level *j=7*. This kind of plots is called Energy Distribution Plots (EDPs). The high value *d=7* in both current and potential reflect the fact that transients with a large frequency prevail over those with small frequency in the original signal. Moreover the high value for *s=7* tell us that the intensity of the trend is bigger than the intensity of the transients in both signal, but more pronounced in the current signal. It can be seen that the maximum relative energy is defined at the smooth *s=7* coefficients while the energy fraction of *d* series is closely to zero, whit exception of d6 and *d7*. While for the potential, energy fractions are not as close to zero.

It is widely accepted that the initiation of pitting commonly occurs prior to other types of localized corrosion, and is much faster than other processes such as diffusion of aggressive species or desorption of corrosion products. Whereby, the relative energy distribution in *d* series it is the dominating and reflects the information about the initiation process of pitting. However, from Fig. 3, it can be seen that the contribution of the smooth *s7* coefficients to the overall signal is sufficiently large to contain information about *d* series crystals, which is associated to the direct current (DC) shift; consequently, the EDP was replotted eliminating the contribution of *s7* crystal from the set signal energy [22].

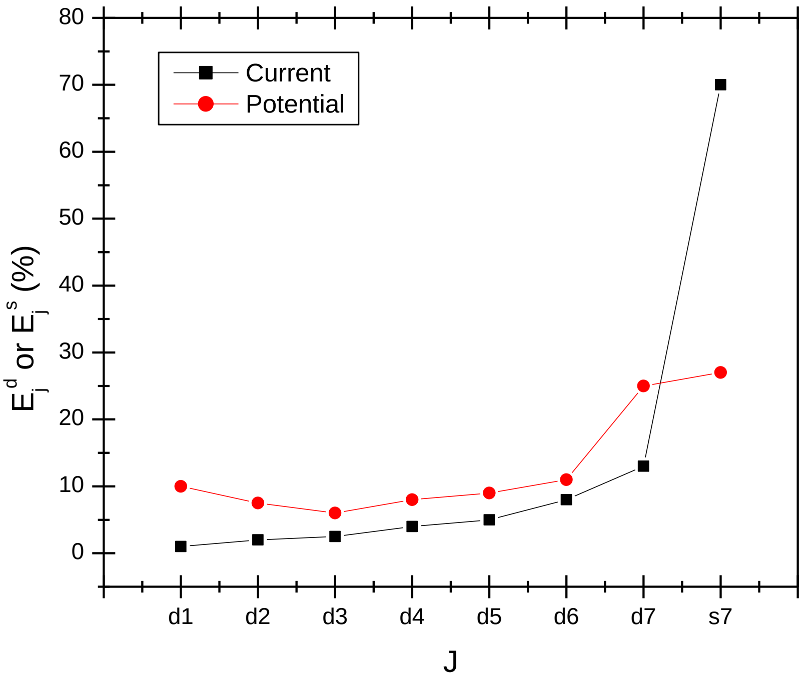

Figure 3. EDPs corresponding to the ECN in Fig. 1.

Analyzing the results of DWT in relation with the noise resistance quantity R_{sn}, it can use the definition of noise resistance based on DWT given by the following equation [9]:

$$R_n(J) = \frac{\sigma(H_{V,J})}{\sigma(H_{C,J})}, \quad (7)$$

where $H_{V,J}$ and $H_{C,J}$ represent the sum of all detail coefficients of the potential (V) and current (I) noise below level J, respectively. σ represents the standard deviation. In Fig. 4 is showed the plot of noise resistance $R_n(J)$ for each accumulated level J. It can be observed that $R_n(J)$ decrease monotonically with the increasing J until reach its minimum value at R_n which is the noise resistance of the overall signal $x_n(t)$.

Fig 4. Shows the plot of noise resistance $R_n(J)$ vs the level J. It can be seen that the $R_n(J)$ decreases exponentially with the decreasing J except for the last value R_n which is the noise resistance of $x_n(t)$. According to Eq. (1), the wavelet scale j may be interpreted as $\frac{t-2^{jk}}{2^j}$ frequency. Apparently, this value decreases with increasing j. Therefore, the reason for the decrease of $R_n(J)$ with j is possibly similar to that for the increase of $R_{sn}(f)$ with decreasing frequency f. Although the relationship between $R_n(J)$ and $R_{sn}(f)$ is unclear. For instance, the $R_n(J)$ in low frequency may be related to the charge transfer process in metastable pitting, the $R_n(J)$ in high frequency may be related to the total metal process [23].

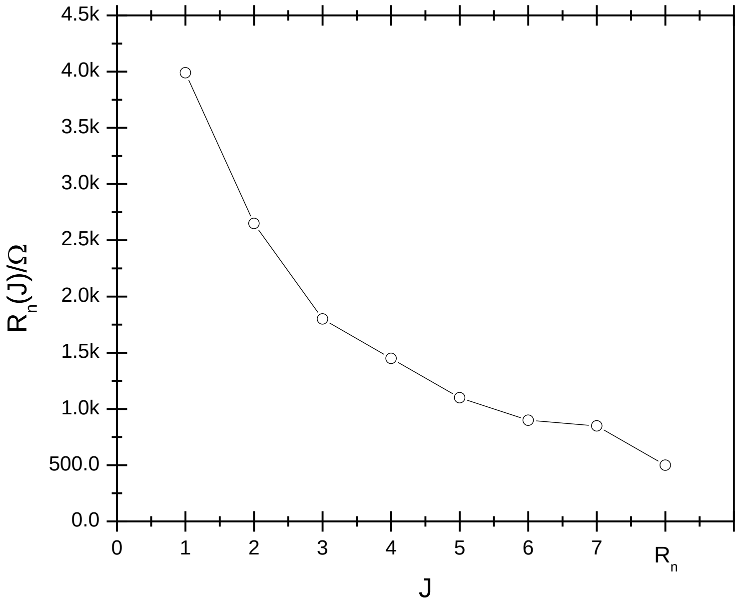

Figure 4. Level accumulated of the noise resistance corresponding to the ECN in Fig. 1.

5. CONCLUSIONS

1. With the experimental conditions shown in this investigation, the characteristics of the energy distribution plots obtained from DWT technique can be used as mathematic model of electrochemical noise signal and for this case, can be used to localized corrosion, corrosion mechanism shown in the results of electrochemical noise technique.

2. The use of DWT technique without observed distortion on signals, can remove the non-linear trend in noise.

3. The experimental results demonstrated that the DWT technique could improve the calculation of the classic noise resistance R_{sn}(f) because it could remove the low frequency trend coupled in the potential or current fluctuations very well.

4. It is noted that the coating used in this study shows good results both in low temperatures in an acid medium [24], as well as high temperature molten salts.

References

1. Ewa Beltowska-Lehman, *Surf. Coat. Technol.,* (2002) 440–443.
2. R. Darolia, *JOM.*, 43 (3) (1991) 4–49.
3. E. P. Busso, F. A. Mcclintock, *Acta Metall. Mater*. 42 (1994) 3263–3275.
4. R. Jayaram, M. K. Miller, *Acta. Metall. Mater*. 42 (1994) 1561–1572.
5. R. D. Field, D. F. Lahrman, R. Darolia, *Acta Metall. Mater*. 39 (1991) 2951–2959.
6. J. Castrejon, S. Serna, A. Wong-Moreno, A. Fragiel, D. Lopez-Lopez, *Mater. Sci. Eng., A,* 415 (2006) 118–125.

7. A. Aballe, M. Bethencourt, F.J. Botana, M. Marcos, *Electrochem. Commun.*, 1 (1999) 266–270.
8. U. Bertocci, J. Frydman, C. Gabrielli, F. Huet, M. Keddam, *J. Electrochem. Soc.*, 145 (1998) 2780.
9. Zehua Dong, Xingpeng Guo, Jiashen Zheng, Liming Xu, *Electrochem. Commun.* 3 (2001) 561-565.
10. F. Mansfeld, Z. Sun, C.H. Hsu, A. Nagiub, *Corros. Sci.* 43 (2001) 341-352.
11. C. Cuevas-Arteaga, J. Porcayo Calderón, *Mater. Sci. Eng., A*, 435-436 (2006) 439-446.
12. M.A. Lucio-Garcia, J.G. Gonzalez-Rodriguez, M. Casales, L. Martinez, J.G. Chacon-Nava, M.A. Neri-Flores, A. Martinez-Villafañe, *Corros. Sci.*, 51 (2009) 2380-2386.
13. F. Mansfeld, Z. Sun, Corrosion, 55 (1999), ProQuest Science Journals, 915.
14. Y. J. Tan, S. Bailey and B. Kinsella, *Corros. Sci.*, 38, 10, (1996) 1681-1695.
15. V. Brusamarello, A. Lago, C.V. Franco, *Corrosion*, 56 (2000) 273.
16. B.B. Hubbard, *The World According to Wavelets*, A.K. Peters, Wellesley, 1996.
17. I. Daubechies, Ten Lectures on Wavelets, Society for Industrial and Applied Mathematics, Philadelphia, PA, 1992.
18. A. Bruce, H.-Y. Gao Applied Wavelet Analysis with S-Plus, Springer, New York, 1996.
19. A. Aballe, M. Bethencourt, F.J. Botana, M. Marcos, *Electrochim. Acta*, 44 (1999), 4805-4816.
20. A. Cohen, I. Daubechies, P. Vial, *Appl. Comput. Harmonic Anal.*, 1 (1993) 54.
21. F. Mansfeld, C.C. Lee, G, Zhang, *Electrochim. Acta*, 43 (1998) 435.
22. F. H. Cao, Z. Zhang, J. X. Su, Y. Y. Shi, J. Q. Zhang, *Electrochim., Acta* 51 (2006) 1359-1364.
23. Zehua Dong, Xingpeng Guo, Jiashen Zheng, Liming Xu, *Electrochem. Commun.* 3 (2001) 561-565.
24. E.F. Diaz, S. Serna, J. Porcayo-Calderon, C. Cuevas, A. Torres Islas, A. Molina, J. Colin, *Int. J. Electrochem. Sci.*, 8 (2013) 7156-7174.

© 2016 The Authors. Published by ESG (www.electrochemsci.org). This article is an open access article distributed under the terms and conditions of the Creative Commons Attribution license (http://creativecommons.org/licenses/by/4.0/).